Photorefractive ring resonators with vectorial two-beam coupling: Theory and applications

Milan Petrović[1] and Milivoj Belić[1,2]
[1]*Institute of Physics, P.O. Box 57, 11001 Beograd, Yugoslavia*
[2]*Department of Physics, Texas A&M University, College Station, Texas 77843*
(Received 9 August 1994; revised manuscript received 9 January 1995)

Oscillation conditions for unidirectional ring resonators containing cubic photorefractive crystals are analyzed. The coupling of pump beams to intracavity modes is presumed to occur via the vectorial two-beam coupling in the crystal. It is also presumed that the intracavity field as well as the pump field are composed of two orthogonally polarized components. The solution of slowly varying envelope wave equations in the degenerate and steady-state limit is used to determine the grating action and to derive threshold conditions for both the transmission and the reflection geometry of the wave-mixing process. A number of special cases of wave-mixing coupling constants is considered. Potential applications of two-wave mixing rings in different photorefractive devices, such as optical amplifiers, switches, and logic circuits are discussed.

PACS number(s): 42.65.Hw, 42.79.Ta

I. INTRODUCTION

The field of optical computing is coming of age [1]. The subject is now a few decades old; however, the visions of powerful all-optical computers with parallel processing, high interconnectivity, and associative memories are still in the distant future. Part of the problem is that electronics works so well. Another part is that optical devices promise so much (parallelism, interconnectivity, high densities, etc.), yet when it comes to implementation most of that remains promises. Nevertheless, optical technology capable of competing with, or even outperforming, electronic circuits is emerging [2]. However, the goal of completely replacing electronic computers with optical ones is not sensible. A hybrid optoelectronic approach seems to be more realistic, in which electronic circuits approaching operational bottlenecks (such as interconnections) are replaced by more powerful optical circuits. It is expected that some parts of future computers (such as memory and logic) will be based on optics, hence the need to develop optical processing units that are functionally analogous to the well-known electronic devices.

Photorefractive (PR) optics [3] may fill part of these needs. The advantages of PR materials are low power consumption, strong beam coupling at low power levels, and parallel processing. Their chief disadvantage is sluggishness at low power levels. Another problem is the poor understanding of wave mixing in such media. Traditionally, experimentation in PR optics leads, with theory lagging behind. We try to address these problems by considering wave-mixing processes in fast cubic PR crystals, and by solving the corresponding wave-mixing equations in a clear and systematic way. Of the various PR optical devices, most promising for applications in optical computing appear to be PR unidirectional rings.

Ring resonators containing PR crystals have proven their utility in the construction and operation of various PR circuits [3,4]. Two interconnected rings with two-wave-mixing (2WM) crystals have been used to display an optical analog of the flip-flop circuit [5]. A simple ring with a single four-wave-mixing (4WM) crystal is shown to operate analogously to a bipolar junction electronic transistor [6]. A 4WM PR crystal can be considered as an eight-pin optical processor [7]. Far-reaching potential applications for PR ring oscillators are thus opening up in the field of optical computing. Therefore, it seems useful to try to better understand the operation of such devices.

From a theoretical point of view a greater understanding of the operation of PR ring resonators has been provided by Yeh [3,8]. An initial analysis of oscillation conditions for unidirectional rings can be found in Ref. [9]. A unified picture of 2WM rings with cross-polarization interaction and 4WM rings with parallel polarization interaction is presented in our earlier publication [10]. There we pointed out symmetries and symmetry breaking between these two classes of ring oscillators, as well as between the transmission and the reflection geometry of wave-mixing processes in such rings.

A crucial problem in the operation of PR oscillators is the slowness of PR crystals. The relaxation time of typical ferroelectric oxides (such as barium titanate) varies inversely with the total illumination intensity, and is of the order of 1 s for milliwatt lasers with beam waists of the order of 1 mm. For ordinary 2WM and 4WM processes, about the only way to speed up the interaction is to use higher intensities. Another problem associated with the operation of PR crystals is inherent instabilities, due to strong nonlinearities. A possible way around these problems is to use cubic PR crystals (such as gallium arsenide) that are not as strongly coupling, yet are a few (3–4) orders of magnitude faster than the ferroelectric crystals operating at comparable power levels.

An additional interesting feature is the vectorial nature of wave coupling in these crystals. This means that if two beams with two orthogonal polarization components (s and p) intersect inside the crystal, then each component

of one beam is coupled to both components of the other beam. The theory and an initial analysis of slowly varying envelope wave equations of vectorial 2WM in cubic PR crystals was performed by Fischer *et al.* [11] and by Yeh [12]. In a recent article [13], we obtained analytical solutions to vectorial 2WM for both the transmission and the reflection geometry of the process. Here we use an alternative method (though similar in spirit) in discussing the oscillation conditions of unidirectional rings with the vectorial coupling of beams. In another recent article [10], we treated a special case of unidirectional rings with the vectorial coupling—that of the cross-polarization coupling. Here the analysis is generalized.

We analyze oscillation conditions for unidirectional ring resonators containing cubic PR crystals of the $\bar{4}3m$ point symmetry as optical elements. The coupling of pumps to the intracavity modes is achieved through the vectorial beam mixing, and we separately discuss the special cases of parallel polarization coupling, of cross-polarization coupling, and of mixed polarization coupling. Also, for greater clarity of presentation, we separately treat the two possible geometries of the wave-mixing process: the transmission geometry (TG) and the reflection geometry (RG). We discuss various potential applications of 2WM PR rings.

The geometries of interest are presented in Fig. 1. The wave equations of interest, describing wave-mixing processes in the crystal, are of the following form:

$$IA_s'=\sigma Q(g_pB_s+g_cB_p),\quad IA_p'=\sigma Q(g_cB_s+g_pB_p)\ , \tag{1a}$$

$$IB_s'=\bar{Q}(g_pA_s+g_cA_p),\quad IB_p'=\bar{Q}(g_cA_s+g_pA_p)\ , \tag{1b}$$

where $I=I_A+I_B$ is the total intensity, and A_s, A_p, B_s, and B_p are the polarization components of the two mixing beams. The prime is the derivative in the propagation (z) direction and $\sigma=\pm$ is the parameter controlling the geometry of wave mixing. The TG results when σ is negative, while the RG results when σ is positive. The quantity $Q=A_s\bar{B}_s+A_p\bar{B}_p$ is the grating amplitude induced in the crystal, and g_p and g_c are the parallel and the cross-polarization coupling constants, assumed to be real. Thus we assume that the buildup of gratings in the crystal is dominated by the diffusion of photoexcited charges. We also assume degeneracy, i.e., the pump and the intracavity field oscillate at the same frequency. The bar stands for complex conjugation. Absorption in the crystal is neglected. Equations (1) should be solved subject to given boundary conditions. This solution is presented in Ref. [13]. Here we provide an outline.

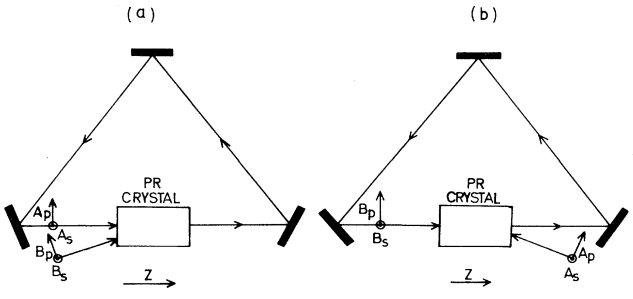

FIG. 1. Ring resonators considered: (a) TG and (b) RG.

The solution of Eqs. (1) is most easily obtained by introducing a new variable θ instead of z,

$$\theta'=\frac{\Gamma|Q|}{I}\ , \tag{2}$$

where Γ is a scaling parameter (given in inverse centimeters). The equations become linear, and the solution is given in terms of sines and cosines for the TG, and in terms of hyperbolic sines and cosines for the RG [13]. The general solution is of the form

$$\begin{bmatrix}A_s\\A_p\\B_s\\B_p\end{bmatrix}=\begin{bmatrix}M_1&\sigma M_2\\M_2&M_1\end{bmatrix}\begin{bmatrix}A_{s0}\\A_{p0}\\B_{s0}\\B_{p0}\end{bmatrix}\ , \tag{3}$$

where the matrix elements are two-by-two matrices,

$$M_1=\begin{bmatrix}c(\theta_p)c(\theta_c)&\sigma s(\theta_p)s(\theta_c)\\\sigma s(\theta_p)s(\theta_c)&c(\theta_p)c(\theta_c)\end{bmatrix}\ , \tag{4a}$$

$$M_2=\begin{bmatrix}s(\theta_p)c(\theta_c)&c(\theta_p)s(\theta_c)\\c(\theta_p)s(\theta_c)&s(\theta_p)c(\theta_c)\end{bmatrix}\ . \tag{4b}$$

The functions $s(x)$ and $c(x)$ denote the sine and cosine in the TG and the hyperbolic sine and cosine in the RG, and $\theta_{p/c}=g_{p/c}(\theta-\theta_0)/\Gamma$. The solution in Eq. (3) is expressed with the help of the initial conditions A_{s0}, B_{s0}, etc. at $z=0$, which is correct for the TG. In the RG, one must reexpress the initial conditions in terms of the given split boundary conditions at $z=0$ and $z=d$, which is a minor algebraic problem. In order to complete the solution, one must determine θ as a function of z from Eq. (2).

To the solutions given by Eq. (3), one must impose cavity oscillation conditions. Even though the noted symmetries between the TG and the RG persist, for greater clarity we prefer to present the TG case and the RG case separately. Thus Sec. II of the paper deals with the TG, Sec. III with the RG. Conclusions and various applications of 2WM rings are given in Sec. IV.

II. TRANSMISSION GEOMETRY

The cavity oscillation condition means that the intracavity field should reproduce itself after each round trip. In the TG, the intracavity field is the A field, so that the conditions read

$$A_{s0}=r\exp(i\psi)A_{sd},\quad A_{p0}=r\exp(i\psi)A_{pd}\ , \tag{5}$$

where r denotes the overall reflectivity of the cavity and ψ is the round-trip phase shift. The subscript d denotes the thickness of the crystal. Assuming that mirror reflections produce a phase shift of ϕ_r, the round-trip phase condition is

$$\psi+\phi_r=2m\pi\ , \tag{6}$$

where m is an integer. In addition to these conditions

there also exist threshold conditions on the coupling strength, which will be investigated in a moment. There also exist frequency conditions, which will not be discussed [8].

The analysis if facilitated by introducing two κ parameters,

$$\kappa_{\pm}=\frac{A_{s0}\pm A_{p0}}{B_{s0}\pm B_{p0}}=\frac{\sin(u_p\pm u_c)}{\cos(u_p\pm u_c)-\dfrac{1}{|r|}}\ , \tag{7}$$

where $u_{p/c}=g_{p/c}(\theta_d-\theta_0)/\Gamma$ is a natural generalization of the grating action $u=\theta_d-\theta_0$ to the case of vectorial coupling. These parameters relate the intracavity field to the pump field. They are very important in our analysis. The latter expression in Eq. (7) is derived using Eqs. (3) and (5). A complete solution to the problem requires the knowledge of both θ as a function of z, and u as a function of boundary conditions. These tasks are most easily accomplished by introducing a couple of auxiliary quantities.

For real coupling constants and no frequency detuning, there is no phase transfer in the process. The phases of beams remain constant in the crystal. There is no phase conjugation in the process either. For such processes there exists an alternative solution procedure involving four specific real quantities: the magnitude of the grating amplitude $|Q|$, the beam flux $F=I_A-I_B$, and two auxiliary quantities,

$$S=A_s\overline{A}_p-B_s\overline{B}_p+\text{c.c.},\quad 2P=A_s\overline{B}_p+A_p\overline{B}_s+\text{c.c.} \tag{8}$$

with no clear physical interpretation. In the remainder, we normalize all quantities with the dimension of intensity to the input pump intensity I_{B0}. One should note that the total intensity I is conserved in the TG,

$$2I_0=(1+a)\kappa_+^2+(1-a)\kappa_-^2+2\ , \tag{9}$$

where $a=(B_{s0}\overline{B}_{p0}+\text{c.c.})/I_{B0}$ is a parameter dependent on the pump beam. There exists a number of other conserved quantities that can be used in the solution process [13]. Here, however, an alternative procedure is followed. In the procedure, $|Q|$ is expressed in terms of the four quantities just introduced,

$$\begin{aligned}2|Q|=&2|Q_0|\cos(2\theta_p)\cos(2\theta_c)+F_0\sin(2\theta_p)\cos(2\theta_c)\\&+S_0\cos(2\theta_p)\sin(2\theta_c)-2P_0\sin(2\theta_p)\sin(2\theta_c)\ ,\end{aligned} \tag{10}$$

and Eq. (2) is solved. The quantities in Eq. (10) can also be expressed in terms of the κ parameters and a,

$$2|Q_0|=(1+a)\kappa_++(1-a)\kappa_-\ , \tag{11a}$$

$$2F_0=(1+a)(\kappa_+^2-1)+(1-a)(\kappa_-^2-1)\ , \tag{11b}$$

$$2S_0=(1+a)(\kappa_+^2-1)-(1-a)(\kappa_-^2-1)\ , \tag{11c}$$

$$2P_0=(1+a)\kappa_+-(1-a)\kappa_-\ . \tag{11d}$$

It should be remembered that all these quantities are scaled with I_{B0}. Even though the integral in the solution of Eq. (2),

$$\Gamma z=2I_0\int_{\theta_0}^{\theta}\frac{d\theta}{2|Q|} \tag{12}$$

cannot be expressed in closed form, for special cases of g_p and g_c, explicit dependence of u on the boundary conditions is found. The evaluation of u sometimes requires the solution of a transcendental equation. We consider four special cases of g_p and g_c: the parallel polarization coupling ($g_p=\Gamma, g_c=0$), the cross-polarization coupling ($g_p=0, g_c=\Gamma$), and the mixed polarization coupling ($g_p=\pm g_c=\Gamma/2$). In all four cases, the modulus of the grating amplitude acquires a general form,

$$2|Q|=A\cos[2(\theta-\theta_0)]+B\sin[2(\theta-\theta_0)] \tag{13}$$

that is convenient for calculations.

A. Parallel polarization coupling

The case $g_p=\Gamma, g_c=0$ is the simplest. The κ become

$$\kappa_+=\kappa_-=\frac{\sin(u)}{\cos(u)-\dfrac{1}{|r|}}\equiv\kappa\ , \tag{14}$$

and the A,B parameters from Eq. (13) are

$$A=2|Q_0|=2\kappa,\quad B=F_0=\kappa^2-1\ . \tag{15}$$

Now Eq. (12) is integrated, and an expression for u found,

$$\tan(u)=\frac{A}{\delta\coth\left[\dfrac{\delta\Gamma d}{2I_0}\right]-B}=\frac{\kappa(b-c)}{b+c\kappa^2}\ , \tag{16}$$

where, by definition,

$$b=\coth(\delta\Gamma d/2I_0)+1,\quad c=\coth(\delta\Gamma d/2I_0)-1\ , \tag{17a}$$

and

$$\delta=(A^2+B^2)^{1/2}=\kappa^2+1\ . \tag{17b}$$

From Eq. (9) it follows that

$$I_0=\kappa^2+1\ , \tag{17c}$$

so that the ratio δ/I_0 is constant. Thus, Eq. (16) represents an explicit equation for u, which is not always true. This is easily seen if κ is eliminated from Eq. (16),

$$\cos(u)=\frac{b+c|r|^2}{|r|(b+c)}\ . \tag{18}$$

A threshold condition on the coupling strength [10] follows from this equation,

$$\tau>|r|\quad\text{for } |r|>1\ , \tag{19a}$$

$$\tau<|r|\quad\text{for } |r|<1\ , \tag{19b}$$

where $\tau=\exp(\Gamma d)=b/c$ is the threshold parameter. Thus, in order to oscillate for $\Gamma d>0$, other active elements must be included in the ring.

The threshold conditions are graphically presented in Fig. 2. As will be seen below, these conditions and the curves are the same for all the special cases, provided one

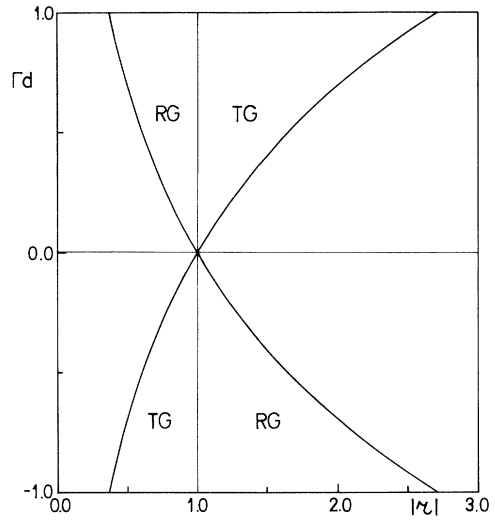

FIG. 2. Threshold conditions presented graphically. The abscissa is the overall reflectivity of the ring, the ordinate is the argument of the exponent in the threshold parameter τ.

chooses the correct argument for the exponential function on the ordinate axis. Actually, there exists a universal argument of the form $(g_p+ag_c)d$, which will be derived later. It is interesting to note the apparent symmetry $\Gamma\rightarrow-\Gamma$ between the TG case and the RG case [introduced by the manner in which Eqs. (1) are written].

B. Cross-polarization coupling

This case, $g_p=0, g_c=\Gamma$, has been covered in our earlier paper [10]. For completeness we list the corresponding formulas. In this case, $\kappa_+=-\kappa_-=\kappa$, where κ is defined above, and

$$A=2|Q_0|=2a\kappa, \quad B=S_0=a(\kappa^2-1) . \tag{20}$$

Furthermore, Eqs. (16) and (18) still hold, with

$$\delta=a(\kappa^2+1), \quad I_0=\kappa^2+1 . \tag{21}$$

Thus, each of the special cases is characterized by its own grating action u. The threshold conditions (19) are also in power, with $\tau=\exp(a\Gamma d)=b/c$. The difference with the parallel polarization case is in the explicit dependence on the pump parameter a.

C. Mixed polarization coupling, the same sign

In this case, $g_p=g_c=\Gamma/2$. The κ parameters are $\kappa_+=\kappa, \kappa_-=0$, and A and B become

$$A=|Q_0|+P_0=(1+a)\kappa , \tag{22a}$$

$$B=\tfrac{1}{2}(F_0+S_0)=\tfrac{1}{2}(1+a)(\kappa^2-1) . \tag{22b}$$

Equations (16) and (18) still hold, with

$$\delta=\tfrac{1}{2}(1+a)(\kappa^2+1) , \tag{23a}$$

and

$$I_0=\frac{\kappa^2}{2}(1+a)+1 . \tag{23b}$$

Now Eq. (16) [or Eq. (18)] represents a transcendental equation for u (both sides of the equation depend on u). The ratio $b/c=\exp(\delta\Gamma d/I_0)$ does not represent the threshold parameter anymore, since δ/I_0 depends on κ. The threshold parameter is obtained by a small u expansion in Eq. (16), with the result $\tau=\exp[(1+a)\Gamma d/2]$. Then the threshold conditions in the form of Eqs. (19) still hold.

D. Mixed polarization coupling, the opposite sign

Now $g_p=-g_c=\Gamma/2$, so that $\kappa_-=\kappa, \kappa_+=0$, and

$$A=|Q_0|-P_0=(1-a)\kappa , \tag{24a}$$

$$B=\tfrac{1}{2}(F_0-S_0)=\tfrac{1}{2}(1-a)(\kappa^2-1) . \tag{24b}$$

Furthermore, Eqs. (16) and (18) are valid, with

$$\delta=\tfrac{1}{2}(1-a)(\kappa^2+1), \quad I_0=\frac{\kappa^2}{2}(1-a)+1 . \tag{25}$$

Again, the threshold parameter is found by a small u expansion in Eq. (16), $\tau=\exp[(1-a)\Gamma d/2]$. Likewise, the threshold conditions (19) are still in power. As is seen, the change $g_c\rightarrow-g_c$ corresponds to a changing of the sign of $a, a\rightarrow-a$; and this is equivalent to introducing a phase shift of π in the phase difference between the pump polarization components B_s and B_p, $\alpha\rightarrow\alpha+\pi$.

A general expression for the threshold parameter is found if one makes a small $\theta-\theta_0$ expansion in Eq. (2), and then solves the equation. The result is of the form

$$\tau=\exp[(g_p+ag_c)d] . \tag{26}$$

Evidently, a high degree of symmetry exists between different cases. This symmetry will be carried over to the RG case as well. Different results for the TG are collected in Table I. Universal quantities that have the same form in all the cases are the κ given by Eq. (14), $\tan(u)$ given by Eq. (16), and $\cos(u)$ given by Eq. (18).

The quantity of special interest is the intracavity oscillation field. A universal parameter used in writing the intracavity field is the amplification coefficient β,

$$\beta=\frac{1-\dfrac{\tau^2}{|r|^2}}{1-|r|^2} . \tag{27}$$

In the parallel polarization case, the s component of the intracavity field is amplified by the s component of the pump, and likewise for the p components,

$$|A_{sd}|^2=\beta|B_{s0}|^2, \quad |A_{pd}|^2=\beta|B_{p0}|^2 . \tag{28a}$$

For the pure cross-polarization coupling, A_{sd} is the amplified B_{p0}, and A_{pd} is the amplified B_{s0},

$$|A_{sd}|^2=\beta|B_{p0}|^2, \quad |A_{pd}|^2=\beta|B_{s0}|^2 . \tag{28b}$$

For the mixed cases, both polarization components are the same, and for the same sign they are given with

TABLE I. Different quantities describing vectorial two-wave mixing in TG, for different combinations of the coupling constants considered in the text. The quantities κ, δ, b/c, and τ are defined in Eqs. (14), (17a), (17b), and (19), respectively.

TG	$g_p=\Gamma, g_c=0$	$g_p=0, g_c=\Gamma$	$g_p=g_c=\Gamma/2$	$g_p=-g_c=\Gamma/2$
$\kappa_\pm$	$\kappa_+=\kappa_-=\kappa$	$\kappa_+=-\kappa_-=\kappa$	$\kappa_+=\kappa, \kappa_-=0$	$\kappa_+=0, \kappa_-=\kappa$
2δ	$2(\kappa^2+1)$	$2a(\kappa^2+1)$	$(1+a)(\kappa^2+1)$	$(1-a)(\kappa^2+1)$
b/c	$\exp(\Gamma d)$	$\exp(a\Gamma d)$	$\exp\left[\frac{\delta}{I_0}\Gamma d\right]$	$\exp\left[\frac{\delta}{I_0}\Gamma d\right]$
τ	$\exp(\Gamma d)$	$\exp(a\Gamma d)$	$\exp\left[\frac{1+a}{2}\Gamma d\right]$	$\exp\left[\frac{1-a}{2}\Gamma d\right]$

$$|A_{sd}|^2=|A_{pd}|^2=\frac{\kappa^2}{4|r|^2}|B_{s0}+B_{p0}|^2 . \tag{28c}$$

For the opposite sign we have

$$|A_{sd}|^2=|A_{pd}|^2=\frac{\kappa^2}{4|r|^2}|B_{s0}-B_{p0}|^2 . \tag{28d}$$

In the section on conclusions, we discuss some of the potential applications of these results.

III. REFLECTION GEOMETRY

A high degree of symmetry exists between the reflection geometry and the transmission geometry of the process, as well as between different special cases. We concentrate on the differences, which are the consequence of different underlying symmetries of the TG and the RG. These symmetries are SU(2) in the case of the TG and SU(1,1) in the case of the RG.

Here we switch the notation, so that now the B field is the intracavity field and the A field is the pump. The oscillation conditions read

$$B_{s0}=r\exp(i\psi)B_{sd},\quad B_{p0}=r\exp(i\psi)B_{pd} , \tag{29}$$

while the κ parameters are

$$\kappa_\pm=-\frac{B_{s0}\pm B_{p0}}{A_{sd}\pm A_{pd}}=\frac{\sinh(u_p\pm u_c)}{1-\frac{\cosh(u_p\pm u_c)}{|r|}} . \tag{30}$$

The round-trip phase condition (6) is assumed to be in effect. The four auxiliary quantities are slightly different now. They are the magnitude of the grating $|Q|$, the total intensity I, and the S and the P, given by

$$S=A_s\bar{A}_p+B_s\bar{B}_p+\text{c.c.},\quad 2P=A_s\bar{B}_p+A_p\bar{B}_s+\text{c.c.} \tag{31}$$

In order to proceed along the lines charted before, one needs the missing boundary values of the A field at $z=0$, written in terms of the given boundary values. These expressions require another pair of parameters,

$$2A_{s0}=(A_{sd}+A_{pd})\chi_+ +(A_{sd}-A_{pd})\chi_- , \tag{32a}$$

$$2A_{p0}=(A_{sd}+A_{pd})\chi_+ -(A_{sd}-A_{pd})\chi_- . \tag{32b}$$

The additional χ parameters also depend on the grating action

$$\chi_\pm=\frac{1+\kappa_\pm\sinh(u_p\pm u_c)}{\cosh(u_p\pm u_c)} . \tag{33}$$

Thus, a complete description of the RG case requires two pairs of parameters, a pair of κ and a pair of χ. The expression for $|Q|$ is analogous to Eq. (10),

$$\begin{aligned}2|Q|=&2|Q_0|\cosh(2\theta_p)\cosh(2\theta_c)\\&+I_0\sinh(2\theta_p)\cosh(2\theta_c)\\&+S_0\cosh(2\theta_p)\sinh(2\theta_c)\\&+2P_0\sinh(2\theta_p)\sinh(2\theta_c) ,\end{aligned} \tag{34}$$

where

$$2|Q_0|=-(1+a)\kappa_+\chi_+-(1-a)\kappa_-\chi_- , \tag{35a}$$

$$2I_0=(1+a)(\kappa_+^2+\chi_+^2)+(1-a)(\kappa_-^2+\chi_-^2) , \tag{35b}$$

$$2S_0=(1+a)(\kappa_+^2+\chi_+^2)-(1-a)(\kappa_-^2+\chi_-^2) , \tag{35c}$$

$$2|P_0|=-(1+a)\kappa_+\chi_++(1-a)\kappa_-\chi_- . \tag{35d}$$

Again, everything is scaled with the pump intensity I_{Ad}. The parameter a is also connected with the pump,

$$a=\frac{A_{sd}\bar{A}_{pd}+\text{c.c.}}{I_{Ad}}=\frac{2|A_{sd}||A_{pd}|\cos(\alpha)}{|A_{sd}|^2+|A_{pd}|^2} . \tag{36}$$

Thus far the differences between the TG and the RG are rather formal. More consequential differences are caused by the fact that I is not conserved in the RG (though F is). The expression for I in the RG is given by

$$\begin{aligned}I=&I_0\cosh(2\theta_p)\cosh(2\theta_c)\\&+2|Q_0|\sinh(2\theta_p)\cosh(2\theta_c)\\&+2P_0\cosh(2\theta_p)\sinh(2\theta_c)\\&+S_0\sinh(2\theta_p)\sinh(2\theta_c) .\end{aligned} \tag{37}$$

This makes the solution of Eq. (2),

$$\Gamma z=\int_{\theta_0}^{\theta}\frac{Id\theta}{|Q|} , \tag{38}$$

more complicated. Similar to Eq. (12), the quadrature in Eq. (38) cannot be expressed in terms of elementary functions for arbitrary g_p and g_c. Below we present a few spe-

cial cases (corresponding to the cases considered in the TG). Before presenting them, we note that the expressions for $|Q|$ and I can be put in more convenient forms,

$$2|Q| = A\cosh[2(\theta-\theta_0)]+B\sinh[2(\theta-\theta_0)] , \tag{39a}$$

$$I = C\cosh[2(\theta-\theta_0)]+D\sinh[2(\theta-\theta_0)]+E , \tag{39b}$$

which are useful in the solution of Eq. (38).

A. Parallel coupling

The case $g_p=\Gamma$ is again the simplest. We have

$$\kappa_+=\kappa_-=\frac{\sinh(u)}{1-\dfrac{\cosh(u)}{|r|}}\equiv\kappa , \tag{40a}$$

$$\chi_+=\chi_-=\frac{1+\kappa\sinh(u)}{\cosh(u)}\equiv\chi . \tag{40b}$$

The A through E parameters from Eqs. (39) become simple functions of κ and χ, and the integration of Eq. (38) is easy. An implicit expression for u follows:

$$\Gamma d = \ln\left|\cosh(2u)-\frac{\kappa^2+\chi^2}{2\kappa\chi}\sinh(2u)\right| . \tag{41}$$

This expression can be simplified to the form

$$\sinh(u)=\frac{\kappa(b-c)}{b+c\kappa^2} , \tag{42}$$

with $b/c=\exp(-\Gamma d)$. This equation is the analog of Eq. (16) in the TG case. Upon eliminating κ from Eq. (42) one finds

$$\operatorname{sech}(u)=\frac{b+c|r|^2}{|r|(b+c)} , \tag{43}$$

which is the analog of Eq. (18). The threshold parameter is $\tau=\exp(-\Gamma d)=b/c$, exactly the inverse of the TG case. However, the conditions following from Eq. (43) are also the inverse. Thus, the threshold conditions given by Eqs. (19) are still in power. One sees that the threshold conditions for the RG are obtained formally from the threshold conditions for the TG by making a transformation $\Gamma\rightarrow-\Gamma$.

B. Cross coupling

For the case $g_c=\Gamma$, the κ and χ are $\kappa_+=-\kappa_-=\kappa$, $\chi_+=\chi_-=\chi$, and the integration of Eq. (38) leads to

$$a\Gamma d = \ln\left|\cosh(2u)-\frac{\kappa^2+\chi^2}{2\kappa\chi}\sinh(2u)\right| . \tag{44}$$

Equation (42) follows, with $b/c=\exp(-a\Gamma d)$, and the threshold parameter has the same form as before. The threshold conditions are also the same. Similar to TG, the only difference with the parallel coupling case is in the explicit dependence on a.

C. Mixed coupling, the same sign

For the case $g_p=g_c=\Gamma/2$ we have $\kappa_+=\kappa$, $\kappa_-=0$ and $\chi_+=\chi$, $\chi_-=1$. The integration of Eq. (38) is a bit more involved this time. A complicated implicit expression for u is found,

$$\Gamma d = \ln\left|\frac{\kappa-\sinh(u)}{\kappa[1+\kappa\sinh(u)]}\right| + \frac{1-a}{1+a}\frac{\cosh^2(u)}{\kappa^2-2\kappa\sinh(u)-1} \times\ln\left|\frac{\kappa\cosh^2(u)}{[1+\kappa\sinh(u)][\kappa-\sinh(u)]}\right| . \tag{45}$$

This expression cannot be brought to a more convenient (explicit) form of the type of Eq. (18). However, a small u expansion can be made, leading to a simple expression for the threshold parameter $\tau=\exp[-(1+a)\Gamma d/2]$. The threshold conditions from Eqs. (19) are in power.

D. Mixed coupling, the opposite sign

In this case ($g_p=-g_c=\Gamma/2$), the κ and χ are $\kappa_+=0$, $\kappa_-=\kappa$, $\chi_+=1$, and $\chi_-=\chi$. The noted symmetry $a\rightarrow-a$ between the two cases with mixed polarization coupling persists in the RG as well. Thus, the expression for u is the same as Eq. (45), provided $a\rightarrow-a$. Likewise for the threshold parameter.

In the end we list the formulas for the resonator fields for different cases. In the case of parallel coupling we have the parallel amplification,

$$|B_{sd}|^2=\beta|A_{sd}|^2,\quad |B_{pd}|^2=\beta|A_{pd}|^2 , \tag{46a}$$

while in the case of cross coupling we have the cross amplification,

$$|B_{sd}|^2=\beta|A_{pd}|^2,\quad |B_{pd}|^2=\beta|A_{sd}|^2 . \tag{46b}$$

For the mixed coupling both polarization components of the intracavity field are given with

$$|B_{sd}|^2=|B_{pd}|^2=\frac{\kappa^2}{4|r|^2}|A_{sd}+A_{pd}|^2 \tag{46c}$$

for the same sign, and with

$$|B_{sd}|^2=|B_{pd}|^2=\frac{\kappa^2}{4|r|^2}|A_{sd}-A_{pd}|^2 \tag{46d}$$

for the opposite sign.

When one plots the oscillation fields for the TG and the RG cases on the same graph, the mentioned $\Gamma\rightarrow-\Gamma$ symmetry between the TG and the RG comes to the forefront. An example is depicted in Fig. 3. Other examples we presented in our other paper [10]. This symmetry is accidental and not forced by any physical laws. As a matter of fact, the curves in Fig. 3 are not perfectly symmetric, although the threshold values of Γd and the saturation values of the oscillation fields are perfectly symmetric.

Some of the results concerning RG are collected in Table II. We should make some comments. The NE entries in the b/c row mean that there do not exist simple exponential expressions for b/c, as in the TG case. The corresponding entries for τ are obtained by making a

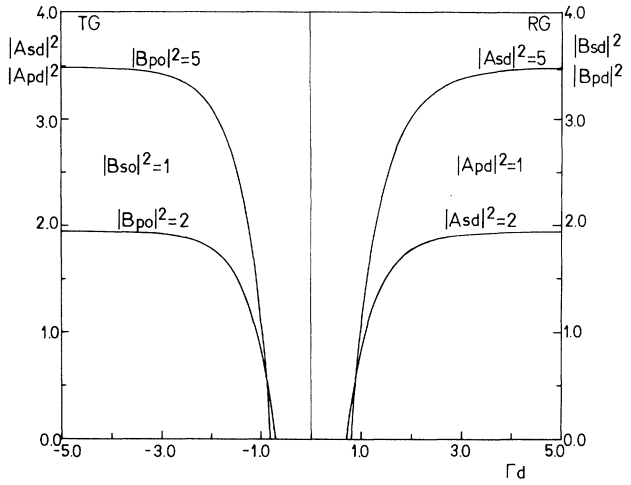

FIG. 3. Intensities of the intracavity oscillating fields as functions of the coupling strength for two values of the pump intensities. The mixed coupling case $g_p=g_c=\Gamma/2$ is considered. Even though the curves for the TG and the RG look perfectly symmetric, this is actually not the case. The existence of a threshold value of Γd for oscillation is clearly visible. The intensity of the other pump component is chosen as the intensity unit. The reflectivity is set at $|r|=0.5$ and the phase difference between the pump components is $\alpha=0$.

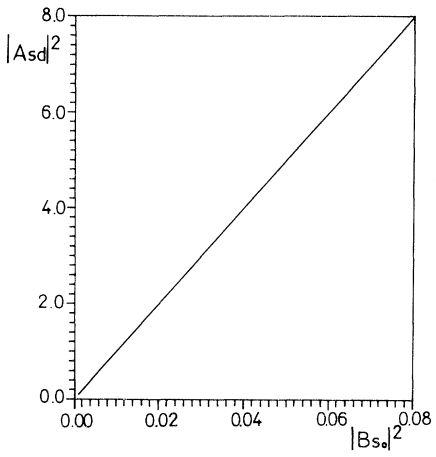

FIG. 4. Amplification in the TG ring with parallel polarization coupling. The parameters are $|r|=0.995$ and $\Gamma d=-5$.

small u expansion in Eq. (45) for both mixed coupling cases. As will be seen below, these approximations are rather good and are useful in the application of rings as logic PR circuits. Results and possible applications are discussed in the next section.

A general expression for the threshold parameter in the RG case is found similarly to the TG case. The result is

$$\tau=\exp[-(g_p+ag_c)d]\ . \tag{47}$$

IV. APPLICATIONS AND CONCLUSIONS

Based on the results derived here and elsewhere [3,10,14] a number of useful PR devices are envisioned. Some of these are mentioned in the Introduction. Yeh and Knoshnevisan proposed a PR ring gyro [15]. Gu and Yeh suggested that a 4WM ring can be used for intensity comparison and thresholding [8]. Unidirectional rings are used for laser beam cleanup [16]. We discovered that a 4WM or 2WM ring with cross-polarization coupling can operate as an optical transistor [6]. Concerning the results obtained here, it should be noted that the transistor action is seen only in the 2WM with cross-polarization coupling, and not in either the parallel or the mixed polarization coupling. It is also seen in 4WM bidirectional rings in both the TG and the RG.

Vectorial 2WM with parallel polarization coupling can be used for optical amplification. With parameters that are not very demanding ($|r|=0.995, \Gamma d=-5$), the amplification coefficient β is of the order of 100. A typical situation is presented in Fig. 4. The other cases of coupling are not convenient for amplification (nor for the transistor action, except the cross-coupling case). This is seen in Fig. 5. The linear response necessary for amplification is achieved only for $\alpha=\pi/2$. On the other hand, vectorial 2WM with cross-polarization coupling can be used for polarization rotation [13]. The material parameters for such an application are very demanding ($\Gamma d\approx 30$).

A useful potential application of the mixed polarization 2WM is for optical switching. To this end one employs the noted symmetry $a\rightarrow -a$, or $\alpha\rightarrow\alpha+\pi$ between the two mixed coupling cases. Starting with the situation where s and p components of the pump are equal in magnitude and are in phase ($\alpha=0$), the switching operation is achieved by turning the "α knob" to the position $\alpha=\pi$, where the fields become out of phase. According to Eqs.

TABLE II. Similar to Table I, except that RG is presented. Instead of the parameter δ (not defined in RG) a new parameter χ appears. The entries NE mean that no simple explicit expressions for b/a exist. The parameters presented are defined in Eqs. (40a), (40b), (42), and (19), respectively.

RG	$g_p=\Gamma, g_c=0$	$g_p=0, g_c=\Gamma$	$g_p=g_c=\Gamma/2$	$g_p=-g_c=\Gamma/2$
$\kappa_\pm$	$\kappa_+=\kappa_-=\kappa$	$\kappa_+=-\kappa_-=\kappa$	$\kappa_+=\kappa, \kappa_-=0$	$\kappa_+=0, \kappa_-=\kappa$
$\chi_\pm$	$\chi_+=\chi_-=\chi$	$\chi_+=\chi_-=\chi$	$\chi_+=\chi, \chi_-=1$	$\chi_+=1, \chi_-=\chi$
b/c	$\exp(-\Gamma d)$	$\exp(-a\Gamma d)$	NE	NE
τ	$\exp(-\Gamma d)$	$\exp(-a\Gamma d)$	$\exp\left[-\frac{1+a}{2}\Gamma d\right]$	$\exp\left[-\frac{1-a}{2}\Gamma d\right]$

(28c), (28d), (46c), and (46d) the intracavity field will switch then from a steady maximum to zero. Thus, by turning one of the polarization components of the pump for 180°, a switch off or a switch on of the resonator field is achieved. The condition for operation of the switch is that the coupling strength Γd is above the oscillation threshold (and below the instability threshold). The notion of instability threshold becomes important when one investigates the temporal behavior of the device. We are in the process of analyzing the dynamical response of various PR ring devices.

The threshold conditions on the coupling strength Γd are very important for the discussion of PR rings. In Fig. 6, we present the threshold values of Γd as a function of the pump beam ratio $q=|B_{s0}|^2/|B_{p0}|^2$. The curves are obtained by putting the equality sign on the threshold conditions in Eqs. (19), $\tau=|r|$. Actually, the implicit relations

$$\Gamma d\left[\frac{1}{2}+\frac{\cos(\alpha)}{q^{1/2}+q^{-1/2}}\right]=\ln|r| \tag{48}$$

are plotted for different values of $|r|$. These graphs should be compared with the similar graphs of Gu and Yeh [8].

A most interesting example of PR ring applications is for optical logic circuits. One can argue that having found an optical transistor, it should not be difficult to connect them into logic circuits. This is not the path we followed. We note that simple 2WM rings as such are the most natural logic circuits. They contain all the necessary ingredients for logic circuits and, by adjusting

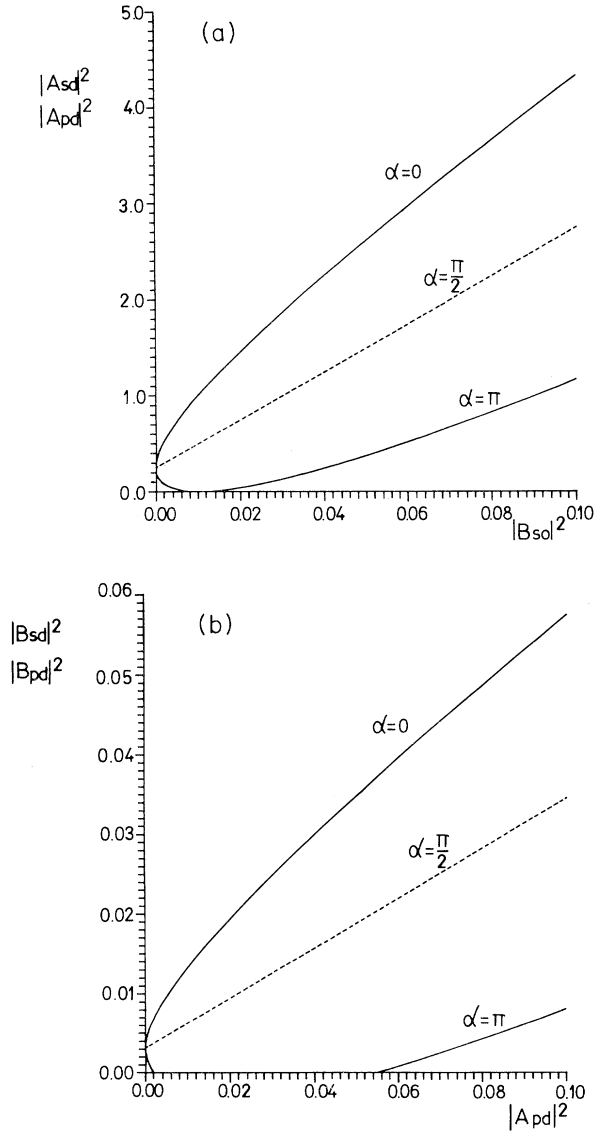

FIG. 5. Amplification in (a) the TG and (b) the RG ring with mixed polarization coupling, for different values of the phase difference α. The parameters for the TG are as in Fig. 4. The parameters for the RG are $|r|=0.5$ and $\Gamma d=5$. The intensity of the other pump component in both geometries is kept fixed at 0.01 (arbitrary units).

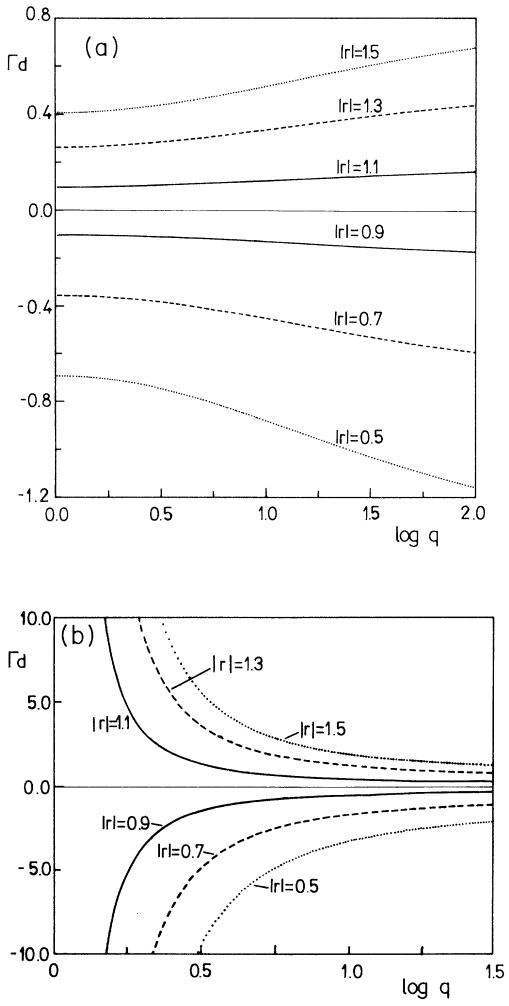

FIG. 6. Threshold value $(\Gamma d)_{\text{th}}$ as a function of the pump components ratio, for different values of $|r|$. Mixed polarization coupling and TG is assumed (a) $\alpha=0$ and (b) $\alpha=\pi$. The base of the log is 10.

the ring parameters, different logic gates can easily be constructed. As before, the pump components are chosen as the input signals and the cavity field components as the output signals.

Another approach to optical digital logic using PR crystals has been advocated by Fainman, Guest, and Lee [17]. They use single crystals (no cavities) and employ three different effects connected with the standard two-beam coupling to demonstrate logic operations. These are the gain saturation, pump depletion, and optically controlled 2WM. The operation of these devices relies on strong couplings in ferroelectric crystals over short distances.

Even though in integrated electronics one prefers to build complicated logic circuits with as few basic logic gates as possible (usually one suffices, the NOR or the NAND gate [18], and other complete sets include the combinations AND, NOT, and OR, NOT), it is not clear in which way the integrated optics will proceed. Therefore, we describe three basic optical logic circuits: OR, AND, and NOT gates. However, before going into detail with these circuits, we present another universally useful PR circuit, the exclusive-or (XOR), gate.

The logic of the XOR optical gate is that the resonator field should be on if one and only one of the input fields is on. It is assumed that the input fields are equal in magnitude. The truth table of the XOR and the other gates is depicted in Fig. 7. The XOR gate is realized with the help of the mixed $g_p = g_c$ ring, the TG case. One uses Eq. (28c) for the oscillation field. The only condition on the parameters is that $\kappa^2/|r|^2 = 4$ should hold. In that case, there is no need to replenish the output field. If either B component is zero, the pump parameter a is zero. The condition is then translated into the following requirement on the reflectivity:

$$(4|r|^2-3)|r|^2 = \exp\left[\frac{4|r|^2+1}{2|r|^2+1}\Gamma d\right] . \tag{49}$$

This condition is easily satisfied for either $\Gamma > 0$ or $\Gamma < 0$. The threshold conditions are also satisfied. For the case when both pump components are on, one chooses $\alpha = \pi$ for the phase difference between the components, and then the cavity field becomes zero. Thus the output is also 0. The XOR gate can be employed in the arithmetic unit of an optical computer. However, a natural photonic application would be for inequality detection or comparison, since the output is only on when $B_{s0} \neq B_{p0}$.

The same PR circuit can be used to realize the NOT gate, provided one of the input beams is used as the ENABLE signal. Thus, for ENABLE=0 the device is inoperative—it just lets the other input signal go through. However, for ENABLE=1 one obtains the negation of the input signal.

The OR gate is obtained using the same circuit if, in addition to $|r|^2$, a condition is set on the phase difference α such that

$$|r|^2[|r|^2-\sin^2(\alpha/2)] = \cos^2(\alpha/2)\exp\left[2\Gamma d\frac{|r|^2+\cos^2(\alpha/2)}{|r|^2+1}\right] . \tag{50}$$

This condition assures that when both inputs are on, the output is also on, and equal in intensity to either of the inputs. Both of these conditions are presented graphically in Fig. 8. The condition on Γd is the same for both the XOR and the OR gate, the condition on α applies only to the OR gate. For the XOR gate $\alpha = \pi$. The existence of a threshold value for $|r|^2$ (equal to 0.75 in this case) is evident from Eq. (49). There also exists a maximum value of $|r|$ for the OR gate (equal to 2.215), that

XOR

B_s	B_p	A
•	•	0
↕	•	1
•	↕	1
↕	↕	0

OR

B_s	B_p	A
•	•	0
↕	•	1
•	↘	1
↕	↘	1

AND

B_s	B_p	A
•	•	0
↕	•	0
•	↕	0
↕	↕	1

FIG. 7. Truth table (with a graphical presentation of the pump components and the phase difference α between them) for different logic circuits considered in the text. (a) Exclusive-or gate, (b) OR gate, and (c) AND gate. The filled dot means zero field.

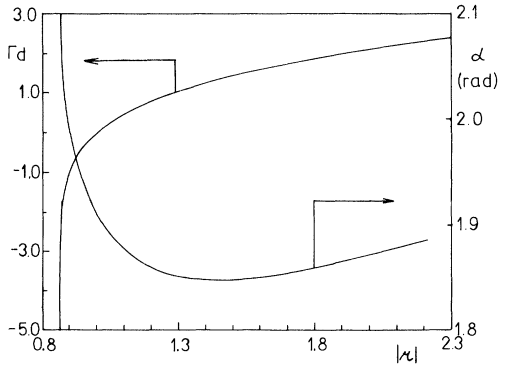

FIG. 8. Conditions on Γd (or $|r|$) and on α for the XOR and OR logic circuits. The curves represent numerical solutions of Eqs. (49) and (50).

follows from Eq. (50).

Other PR circuits can be used to obtain other logic gates. The AND gate can be realized by using the cross-coupling TG ring. The input is still the B_s and B_p components, the output is either A_s or A_p. If the pump components are in phase and $\Gamma < 0$, the threshold condition is $\exp(a\Gamma d) < |r| < 1$. If either of the pump components is zero, $a = 0$, and if $|r|$ is chosen to be smaller than one, the ring is inoperative, because the threshold condition is not satisfied. However, if both pumps are nonzero, the threshold condition is satisfied, and the cavity oscillation is on. This is similar to the threshold logic used elsewhere in optical computing [1]. By choosing, for example, $\Gamma d = -1.4$ and $|r| = 0.5$, one gets $\beta = 1$.

In this manner, far-reaching potential applications of PR rings are envisioned in the field of optical computing. The extension to parallel processing of two-dimensional signal arrays (which is essential for optical computing) should present no principal problem. However, there remains the crucial problem of implementation. One can hope that the materials with the right characteristics will be found, and that useful geometries and PR circuits will be developed. Judging by the present pace in the development of integrated optics and optical computers, we hope that the road from idea to implementation will not be as long and winding.

In summary, we considered the theory of vectorial 2WM in rings containing PR crystals. Oscillation conditions are analyzed for the general case of wave couplings, and for a number of special cases in both the transmission and the reflection geometry of the wave-mixing process. The threshold conditions are derived and the expressions for stationary intracavity fields are given in terms of useful parameters, such as the amplification coefficient and the coupling strength. We then use the results obtained to propose a number of potential applications of PR rings with vectorial two-beam coupling.

It could reasonably be argued that some of the applications proposed are too optimistic. Presently, high gains in cubic crystals are achieved by applying dc voltages to the crystals. When high fields are applied to the crystal, the gain is likely to become nonuniform. Also, the analysis presented here is plane wave, while transverse effects are expected to play an important role in the operation of such optical devices. We are in the process of including transverse and dynamical effects. Nevertheless, we hope that we have pointed out some useful potential applications of PR rings in optical computing.

[1] *Optical Processing and Computing,* edited by H. Arsenault *et al.* (Academic, Boston, 1989); D. Feitelson, *Optical Computing* (MIT, Cambridge, 1988).
[2] IEEE J. Quantum Electron. **QE-29** (2) (1993), special issue on smart pixels, edited by S. R. Forrest and H. S. Hinton.
[3] P. Yeh, *Photorefractive Nonlinear Optics* (Wiley, New York, 1993).
[4] B. Fischer, S. Sternklar, and S. Weiss, IEEE J. Quantum Electron. **QE-25**, 550 (1989).
[5] D. Anderson, C. Benkert, B. Chorbajian, and A. Hermanns, Opt. Lett. **16**, 250 (1991).
[6] M. Belić, M. Petrović, and F. Kaiser (unpublished).
[7] S. L. Wang and H. F. Pan, Opt. Commun. **103**, 116 (1993).
[8] C. Gu and P. Yeh, J. Opt. Soc. Am. B **8**, 1428 (1991).
[9] A. Yariv and S. K. Kwong, Opt. Lett. **10**, 454 (1985).
[10] M. Petrović and M. Belić, J. Opt. Soc. Am. B **12**, xx (1995).
[11] B. Fischer, J. O. White, M. Cronin-Golomb, and A. Yariv, Opt. Lett. **11**, 239 (1986).
[12] P. Yeh, IEEE J. Quantum Electron. **QE-25**, 484 (1989).
[13] M. Petrović and M. Belić, Opt. Commun. **109**, 338 (1994).
[14] *Photorefractive Materials and Their Applications II,* edited by P. Günter and J.-P. Huignard (Springer, Berlin, 1989).
[15] P. Yeh and M. Knoshnevisan, Soc. Photo-opt. Instrum. Eng. **487**, 102 (1984).
[16] S. Kwong and A. Yariv, Appl. Phys. Lett. **48**, 564 (1986).
[17] Y. Fainman, C. Guest, and S. Lee, Appl. Opt. **25**, 1598 (1986).
[18] J. C. Boyce, *Digital Logic and Switching Circuits* (Prentice-Hall, Englewood Cliffs, NJ, 1975).